12th IFToMM World Congress, Besançon (France), June18-21, 2007

# Non-smooth Periodic Dynamics of a Bush in Tribological Conditions

J. Awrejcewicz* Yu. Pyryev†
Technical University of Łódź
Department of Automatics and Biomechanics
Łódź, Poland

**Abstract**—*In this work the model of a contact system with heat and wear generated by friction and/or impacts is studied. The methods and mathematical models of such systems applied so far by others contribute only partially to the description of complex dynamics. First, the analysis of contacting dynamic models omits tribological processes on a contact body surface. Second, the mentioned models do not include either the body inertia or impact phenomena usually appearing within the body clearance. We contribute to the problem by matching both phenomena, which improves modeling of dynamic behavior of contacting bodies. Analysis of both stick-slip and slip-slip motion exhibited by the system is performed (impact-less behavior of this model has already been studied by the authors [1-3]), among the others. Analytically predicted vibro-impact stick-slip and slip-slip dynamics has been also verified numerically.*

**Keywords: friction, impacts, thermo-elasticity, wear**

## I. Introduction

Attention is focused on modeling of non-linear dynamics of two bodies consisting of a stiff bush with clearance $2\Delta_\varphi$ (see Figure 1). The bush is coupled with housing by springs with stiffness $k_2$ and is mounted on the rotating thermo-elastic shaft 1.

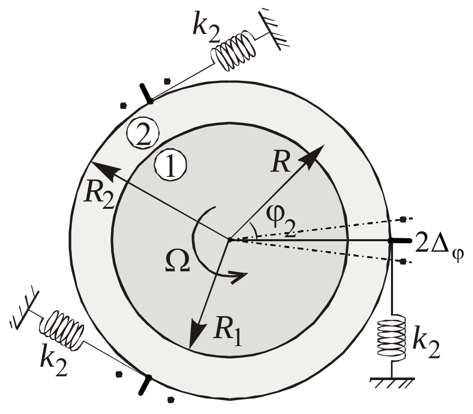


Fig. 1. Analyzed system

The following assumptions are taken: (i) the shaft rotates with such enough small angular velocity $\Omega$ that centrifugal forces can be omitted; (ii) non-linear kinetic friction occurs between the bush and the shaft; (iii) heat is generated on the contacting surface $R = R_1$ due to friction; (iv) heat transfer between contacting bodies is governed by Newton's law.

## II. Equations for shaft rotational movement of an absolutely rigid bush

Let axis $Z$ be a cylinder axis. The equilibrium state of the moments of forces with respect to the shaft axis gives

$$B_2\ddot{\varphi}_2(t) + k_2R_2^2\varphi_2(t) = f(V_r)2\pi R_1^2 P(t)\,,$$

$$|\varphi_2(t)| < \Delta_\varphi\,,\ \dot{\varphi}_2(t) \neq \Omega\ ; \tag{1}$$

$$\ddot{\varphi}_2(t) = 0\,,\ |\varphi_2(t)| < \Delta_\varphi\,,\ \dot{\varphi}_2(t) = \Omega\,; \tag{2}$$

$$\dot{\varphi}_2^+ = -k\dot{\varphi}_2^-\,,\ |\varphi_2| = \Delta_\varphi\,,\ \dot{\varphi}_2^-\varphi_2 > 0\,, \tag{3}$$

where: $V_r = R_1\Omega - R_1\dot{\varphi}_2(t)$ relative velocity of the contact bodies, $k$ is the coefficient of restitution, $\dot{\varphi}_2^-$ ($\dot{\varphi}_2^+$) is the bush velocity just before (after) impact, $B_2$ is the moment of inertia of the bush per length unit, $f(V_r)$ is the kinetic friction coefficient depending on relative velocity, $P(t)$ is the contact pressure. The initial value problem is defined in the following way:

$$\varphi_2(0) = \varphi_2^\circ\,,\ \dot{\varphi}_2(0) = \omega_2^\circ\,. \tag{4}$$

Relation approximating curve $f(V_r)$ has the following form

$$f(V_r) = \mathrm{sgn}(V_r)F(|V_r|)\,,$$

$$F(V_r) = \begin{cases} F_0 - \kappa V_r\,, & 0 < V_r \le V_{\min} \\ F_0 - \kappa V_{\min}\,, & V_{\min} < V_r \end{cases} \tag{5}$$

where: $F_0$, $\kappa$, $V_{\min}$ are constant coefficients.

## III. Thermo-elastic shaft

Inertial terms occurring in the equation of motion are omitted in our study and the problem may be considered as a quasi-static one. In the case of axially symmetric shaft stresses, the governing equations can be derived using theory of thermal stresses for an isotropic body (see Nowacki [4]). Applying cylindrical coordinates one gets the following set of equations

$$\frac{\partial^2 U(R,t)}{\partial R^2} + \frac{1}{R}\frac{\partial U(R,t)}{\partial R} - \frac{1}{R^2}U(R,t) = \alpha_1\frac{1+\nu_1}{1-\nu_1}\frac{\partial T_1(R,t)}{\partial R}\,,$$

* E-mail: awrejcew@p.lodz.pl
† E-mail: jupyrjew@p.lodz.pl

$$\frac{\partial^2 T_1(R,t)}{\partial R^2} + \frac{1}{R}\frac{\partial T_1(R,t)}{\partial R} = \frac{1}{a_1}\frac{\partial T_1(R,t)}{\partial t}\,,\ 0<R<R_1\,, \quad (6)$$

with the attached mechanical

$$U(0,t)=0\,,\ U(R_1,t) = -U_0 h_U(t) + U^w(t)\,, \quad (7)$$

and thermal boundary conditions

$$\lambda_1 \frac{\partial T_1(R_1,t)}{\partial R} + \alpha_T T_1(R_1,t) = (1-\eta) f(V_r) V_r P(t) \quad (8)$$

$$\lambda_1 2\pi R \left.\frac{\partial T_1(R,t)}{\partial R}\right|_{R\to 0} = 0\,, \quad (9)$$

and with the following initial conditions

$$T_1(R,0)=0\,,\ 0<R<R_1\,. \quad (10)$$

Velocity of the bush wear is proportional to a certain power of friction force. According to Archard's assumption [5] we have

$$\dot U^w(t) = K^w |V_r(t)| P(t) \quad (11)$$

where $K^w$ is the coefficient usually identified experimentally.

Shaft radial stresses $\sigma_R(R,t)$ may be found knowing radial displacement $U(R,t)$ and temperature $T_1(R,t)$ from the following formula

$$\sigma_R(R,t) = \frac{E_1}{1-2\nu_1}\left[\frac{1-\nu_1}{1+\nu_1}\frac{\partial U(R,t)}{\partial R} + \frac{\nu_1}{1+\nu_1}\frac{U(R,t)}{R} - \alpha_1 T_1(R,t)\right]$$

The following notation has been applied: $P(t) = -\sigma_R(R_1,t)$ - contact pressure; $U(R,t)$ - displacement component along radial direction in the shaft: $E_1$ - Young modulus; $\nu_1$ - Poisson's ratio; $a_1$ - thermal diffusivity, $\alpha_1$ - thermal expansion coefficient; $\lambda_1$ - thermal conductivity; $K^w$ - wear constant coefficient; $\eta \in [0, 1]$ - denotes the part of heat energy which goes on the wear.

Upon integration of the first equation of (6) and taking into account (7) the contact pressure is

$$P(t) = \frac{2E_1\alpha_1}{1-2\nu_1}\frac{1}{R_1^2}\int_0^{R_1} T_1(\xi,t)\xi d\xi + \frac{E_1}{(1-2\nu_1)(1+\nu_1)R_1}\left[U_0 h_U(t) - U^w(t)\right] \quad (12)$$

## IV. Solution Algorithm

Let us introduce the following dimensionless parameters:

$$\tau = \frac{t}{t_*}\,,\ r = \frac{R}{R_1}\,,\ \varphi(\tau) = \frac{\varphi_2}{\Delta_\varphi}\,,\ p = \frac{P}{P_*}\,,\ \theta = \frac{T_1}{T_*}\,,$$

$$u^w = \frac{U^w}{U_0}\,,\ \alpha_0 = \frac{f_0}{F_0}\,,\ \omega_1 = \frac{\Omega t_*}{\Delta_\varphi} = \frac{1}{\gamma\sqrt{\alpha_0}}\,,\ Bi = \frac{\alpha_T R_1}{\lambda_1}\,,$$

$$\mu_0 = (1-\alpha_0)/\alpha_0\,,\ \varepsilon = \mu_0\gamma\sqrt{\alpha_0} = \mu_0/\omega_1\,,$$

$$\eta_0 = (V_0 - V_{min})/V_0\,,\ h_U(\tau) = h_U(t_*\tau)\,,\ f(V_0) = f_0\,,$$

$$\gamma = \sqrt{\frac{2\pi R_1^2 P_* F_0 \Delta_\varphi}{B_2\Omega^2}}\,,\ \omega_0^2 = \frac{k_2 R_2^2 t_*^2}{B_2}\,,$$

$$k^w = \frac{K^w \Delta_\varphi E_1}{(1-2\nu_1)(1+\nu_1)}\,,\ \gamma_1 = \frac{(1-\eta)E_1\alpha_1 R_1^2 f_0 \Delta_\varphi}{\lambda_1(1-2\nu_1)t_T}\,,$$

$$\tilde\omega = \frac{t_*}{t_T}\,,\ \Psi = \frac{F}{f_0}\,,\ x = \frac{\overset{\circ}{\varphi}_2}{\Delta_\varphi}\,,\ y = \frac{\overset{\circ}{\omega}_2 t_*}{\Delta_\varphi}\,, \quad (13)$$

where:

$$t_* = \sqrt{\frac{B_2\Delta_\varphi}{f_0 2\pi R_1^2 P_*}}\,,\ V_* = \frac{R_1\Delta_\varphi}{t_*}\,,\ T_* = \frac{U_0}{\alpha_1(1+\nu_1)R_1}\,,$$

$$P_* = \frac{E_1 U_0}{(1-2\nu_1)(1+\nu_1)R_1}\,,\ t_T = \frac{R_1^2}{a_1}\,,\ V_0 = \Omega R_1\,. \quad (14)$$

The dimensionless equations governing dynamics of the analyzed system have the form

$$\ddot\varphi(\tau) + \omega_0^2\varphi(\tau) = \mathrm{sgn}(\omega_1 - \dot\varphi)\Psi(\dot\varphi)p(\tau)\,,$$
$$|\varphi(\tau)|<1\,,\ \dot\varphi(\tau)\neq\omega_1\ ; \quad (15)$$

$$\ddot\varphi(\tau)=0\,,\ |\varphi(\tau)|<1\,,\ \dot\varphi(\tau)=\omega_1\ ; \quad (16)$$

$$\dot\varphi^+ = -k\dot\varphi^-\,,\ |\varphi|=1\,,\ \dot\varphi^-\varphi>0\ ; \quad (17)$$

$$\varphi(0)=x\,,\ \dot\varphi(0)=y\,, \quad (18)$$

where:

$$\Psi(\dot\varphi) = \begin{cases} 1+\varepsilon\omega_1\eta_0, & \dot\varphi<\omega_1\eta_0,\ \omega_1(2-\eta_0)<\dot\varphi \\ 1+\varepsilon\dot\varphi, & \omega_1\eta_0<\dot\varphi<\omega_1 \\ 1+2\varepsilon\omega_1-\varepsilon\dot\varphi, & \omega_1<\dot\varphi<\omega_1(2-\eta_0) \end{cases} \quad (19)$$

In order to solve the motion equations (15) one needs to know contact pressure $p(\tau)$ and wear $u^w(\tau)$:

$$p(\tau) = h_U(\tau) - u^w(\tau) + \int_0^1 \theta(\xi,\tau)\xi\, d\xi\,, \quad (20)$$

$$u^w(\tau) = k^w\int_0^\tau |\omega_1 - \dot\varphi(\tau)| p(\tau)d\tau\,. \quad (21)$$

The one-dimensional transient heat conduction equation under consideration takes the following dimensionless form

$$\frac{\partial^2\theta(r,\tau)}{\partial r^2} + \frac{1}{r}\frac{\partial\theta(r,\tau)}{\partial r} = \frac{1}{\tilde\omega}\frac{\partial\theta(r,\tau)}{\partial\tau} \quad (22)$$

whereas the thermal boundary conditions are

$$\left[\frac{\partial\theta(r,\tau)}{\partial r} + Bi\,\theta(r,\tau)\right]_{r=1} = \gamma_1\tilde\omega^{-1}\,\Psi(\dot\varphi(\tau))|\omega_1 - \dot\varphi(\tau)|p(\tau)\,,$$

$$2\pi r\left.\frac{\partial\theta(r,\tau)}{\partial r}\right|_{r\to 0} = 0 \quad (23)$$

and initial conditions are as follows

$$\theta(r,0)=0\,. \quad (24)$$

Applying an inverse Laplace transformation ([2], [6]), the nonlinear problem governed by Eqs. (22), (23) and (24) is reduced to the following integral equation of the second kind of Volterra type

$$p(\tau) = h_U(\tau) - u^w(\tau) + 2\gamma_1 \tilde{\omega}^{-1} \int_0^\tau \dot{G}_p(\tau-\xi)\Psi(\dot{\varphi}(\xi))\left|\omega_1 - \dot{\varphi}(\xi)\right| p(\xi)d\xi \quad (25)$$

Then the problem is reduced to consideration of equations (15) and (25), which yield both dimensionless pressure $p(\tau)$ and velocity $\dot{\varphi}(\tau)$. The temperature is defined by the following formula

$$\theta(r,\tau) = \gamma_1 \tilde{\omega}^{-1} \int_0^\tau \dot{G}_\theta(r,\tau-\xi)\Psi(\dot{\varphi}(\xi))\left|\omega_1 - \dot{\varphi}(\xi)\right| p(\xi)d\xi,$$

where

$$\left\{G_p(\tau), G_\theta(1,\tau)\right\} = \frac{\{0.5,\ 1\}}{Bi} - \sum_{m=1}^{\infty} \frac{\left\{2Bi,\ 2\mu_m^2\right\}}{\mu_m^2(Bi^2+\mu_m^2)} e^{-\mu_m^2 \tilde{\omega}\tau},$$

and $\mu_m$ are the roots of the characteristic equation

$$BiJ_0(\mu) - \mu J_1(\mu) = 0 .$$

## IV. Analysis

First the case of bush vibrations without tribological processes is studied ($\gamma_1 = 0$, $k^w = 0$). For this case we have $p(\tau) = h_U(\tau)$. Our system governed by equations (15) may exhibit four different periodic motions. Namely: (i) periodic orbit with one impact, where a stick does not appear; (ii) periodic orbit with one impact, where a stick-slip occurs; (iii) periodic orbit with two impacts, where a slip of the contacting bodies occurs; (iv) periodic orbit with two impacts, where a stick-slip appears.

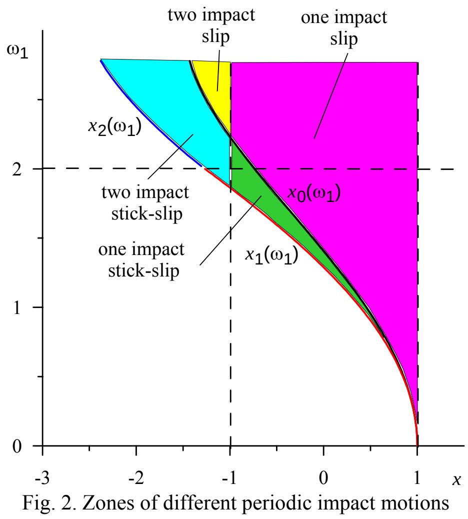

Fig. 2. Zones of different periodic impact motions

In what follows we assume that $\varepsilon << 1$, $\omega_0^2 << 1$, $\omega_0^2 = \delta\varepsilon$, and $\eta_0 \le -1$. It means that the system dynamics is exhibited in the interval ($0 < V_0 < V_{\min}$), where a decreasing slope of the kinetic friction coefficient is observed.

Results of our consideration allow us to give formulas for the coefficient of restitution $k$ for a general case of the following case

$$k(x,\omega_1) = \begin{cases} k_{ACMNA}, & 0<\omega_1<2-(4/3)\varepsilon, \quad x_1<x<x_0 \\ k_{AMNA,} & 0<\omega_1<2-(4/3)\varepsilon, \quad x_0<x<1 \\ k_{BCMNDB}, & 2-(4/3)\varepsilon<\omega_1<2, \quad x_1<x<-1 \\ k_{ACMNA}, & 2-(4/3)\varepsilon<\omega_1<2, \quad -1<x<x_0 \\ k_{AMNA,} & 2-(4/3)\varepsilon<\omega_1<2, \quad x_0<x<1 \\ k_{BCMNDB}, & 2<\omega_1<2+(4/3)\varepsilon, \quad x_2<x<-1 \\ k_{ACMNA}, & 2<\omega_1<2+(4/3)\varepsilon, \quad -1<x<x_0 \\ k_{AMNA,} & 2<\omega_1<2+(4/3)\varepsilon, \quad x_0<x<1 \\ k_{BCMNDB}, & 2+(4/3)\varepsilon<\omega_1<\infty, \quad x_2<x<x_0 \\ k_{BMNDB}, & 2+(4/3)\varepsilon<\omega_1<\infty, \quad x_0<x<-1 \\ k_{AMNA,} & 2+(4/3)\varepsilon<\omega_1<\infty, \quad -1<x<1 \end{cases}$$

where

$$k_{AMNA} = 1-(2/3)\tau_1\varepsilon + o(\varepsilon^2), \quad \tau_1 = \sqrt{2(1-x)},$$

$$k_{BMNDB} = 1 + \frac{\tau_2^3 - \tau_1^3}{3(2+\tau_2^2)}\varepsilon + o(\varepsilon^2), \quad \tau_2 = \sqrt{-2(1+x)},$$

$$k_{ACMNA} = \tau_1/\omega_1 - (1/3)(\tau_1^2/\omega_1)\varepsilon - (1/8)(\tau_1/\omega_1)(4-\tau_1^2)\delta\varepsilon + o(\varepsilon^2),$$

$$k_{BCMNDB} = \frac{\tau_0}{\omega_1} + \frac{-16\tau_0^2 + \tau_2^3\omega_1^2(\tau_0+\omega_1) - \tau_2^2\omega_1^2(4+\tau_0^2)}{6\omega_1(\tau_2^2\omega_1^2 + 2\tau_0^2)}\varepsilon + \frac{\tau_2^2\tau_0\omega_1(\tau_2^2+4)}{16(\tau_2^2\omega_1^2+2\tau_0^2)}\delta\varepsilon + o(\varepsilon^2),$$

$$\tau_0 = \sqrt{2+\sqrt{4+\tau_2^2\omega_1^2}} .$$

The obtained results are graphically presented in Figure 2 where

$$x_0(\omega_1) = 1-(1/2)\omega_1^2 + (1/3)\omega_1^3\varepsilon + (1/8)\omega_1^2(\omega_1^2-4)\delta\varepsilon + o(\varepsilon^2)$$

$$x_1(\omega_1) = 1-0.5\omega_1^2 - (1/3)\omega_1^3\varepsilon + (1/8)\omega_1^2(\omega_1^2-4)\delta\varepsilon + o(\varepsilon^2),$$

$$x_2(\omega_1) = x_1(\omega_1) + (2/3)(\omega_1^2-4)^{3/2}\varepsilon .$$

Observe that the function $k(x,\omega_1)$ possesses the following values $k(x_1,\omega_1)=1$, $2<\omega_1<\infty$, $k(x_2,\omega_1)=1$, $2<\omega_1<\infty$, $k(1,\omega_1)=1$ at the boundaries, whereas inside the considered interval it has the following minima

$$\min_{x\in[x_1,1]} k(x,\omega_1) = k(x_0,\omega_1) = 1-(2/3)\omega_1\varepsilon, \quad 0<\omega_1<2+(4/3)\varepsilon,$$

$$\min_{x\in[x_2,1]} k(x,\omega_1) = k(-1,\omega_1) = 1-(4/3)\varepsilon, \quad 2+(4/3)\varepsilon<\omega_1<\infty$$

which can be presented in the form

$$k_{\min} = \begin{cases} 1-(2/3)\omega_1\varepsilon, & 0<\omega_1<2+(4/3)\varepsilon \\ 1-(4/3)\varepsilon, & 2+(4/3)\varepsilon<\omega_1<\infty \end{cases}. \quad (26)$$

Notice that for an arbitrary $k^* \in (k_{\min},1)$ there are two values of $x_1^*$, $x_2^*$ ($k(x_1^*,\omega_1)=k(x_2^*,\omega_1)=k^*$). Let us introduce the following intervals

$x_1 < x_1^* < x_0, x_0 < x_2^* < 1$ for $0<\omega_1<2$,

$x_2 < x_1^* < x_0, x_0 < x_2^* < 1$ for $2<\omega_1<2+(4/3)\varepsilon$,

$x_2 < x_1^* < -1, -1 < x_2^* < 1$ for $2-(4/3)\varepsilon<\omega_1<\infty$

It is not difficult to check that a periodic orbit associated with $x_1^*$ (decreasing part of the coefficient $k(x)$) is stable, whereas a periodic orbit associated with $x_2^*$ (increasing part of the coefficient $k(x)$) is unstable.

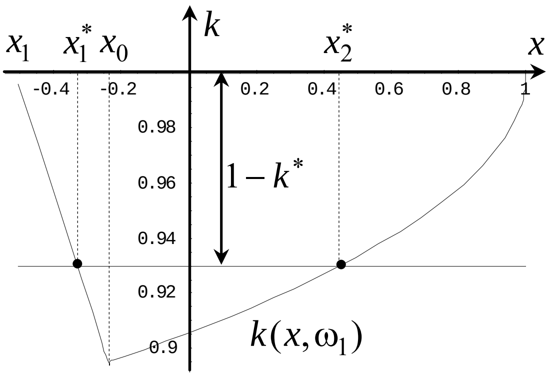


Fig. 3. Graphical solution of equation $k(x,\omega_1)=k^*$

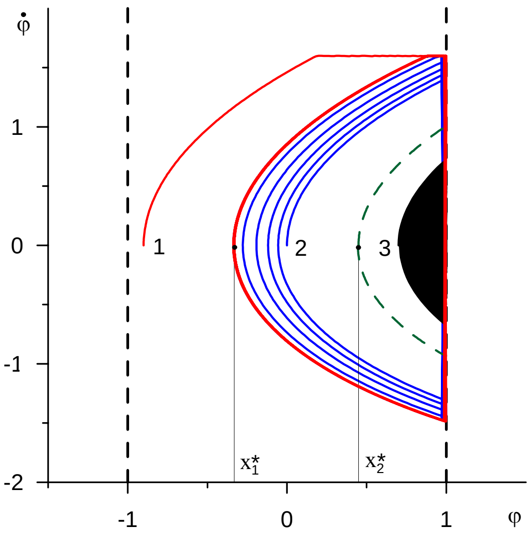


Fig. 4. Phase trajectory of the bush movement for different values of $x$

A numerical analysis has been carried out for the following dimensionless parameters: $\varepsilon=0.1$, $\omega_1=1.6$, $\delta=2$, $\omega_0^2=0.2$. Formula (26) gives $k_{\min}=0.89$. If $k^*=0.93$ ($k^*\in(k_{\min},1)$), then our system exhibits two periodic orbits defined by $x_1^*=-0.33$ (stable) case (ii) and $x_2^*=0.44$ (unstable) case (i) (see Fig. 3 and 4).

Curves 1 and 2 approach a stable periodic orbit, whereas curve 3 tends to the stable point (1,0). Note that the dashed curve is associated with an unstable orbit (see Figure 4). Curves 1 - $x=-0.9$ ($0\le x<x_1^*$), curves 2 - $x=0$ ($x_1^*<x<x_2^*$), curves 3 - $x=0.7$ ($x_2^*<x\le 1$).

Next, a numerical analysis has been carried out for the following dimensionless parameters: $\varepsilon=0.1$, $\omega_1=1.6$, $\omega_0^2=0.2$, $\eta_0=-2$, $\tilde{\omega}=0.1$. For $x=-0.9$ and $k=0.93$ the corresponding bush phase trajectory for various parameters $\gamma_1$ and $k^w$ is shown in Figure 5-8.

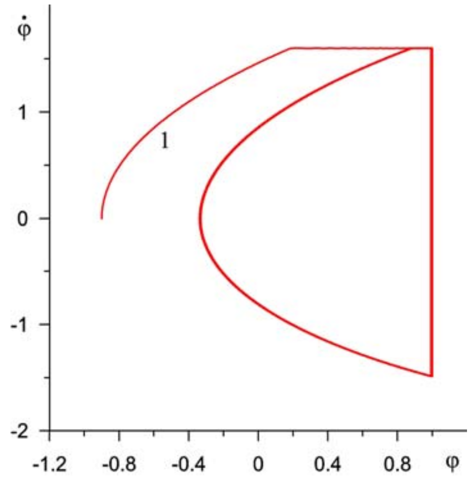


Fig. 5. Phase trajectory of the bush movement for $\gamma_1=0$, $k^w=0$

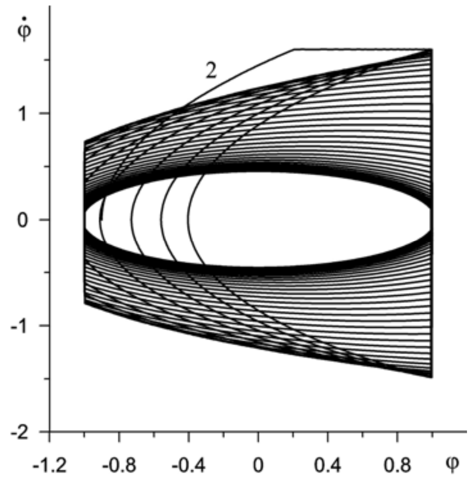


Fig. 6. Phase trajectory of the bush movement for $\gamma_1=0$, $k^w=0.02$

Curves 1 - $\gamma_1 = 0$ , $k^w = 0$ (without tribologic processes), curves 2 - $\gamma_1 = 0$ , $k^w = 0.02$ , curves 3 - $\gamma_1 = 0.1$ , $k^w = 0$ (with heat generation), curves 4 - $\gamma_1 = 0.5$ , $k^w = 0.02$ (with tribologic processes).

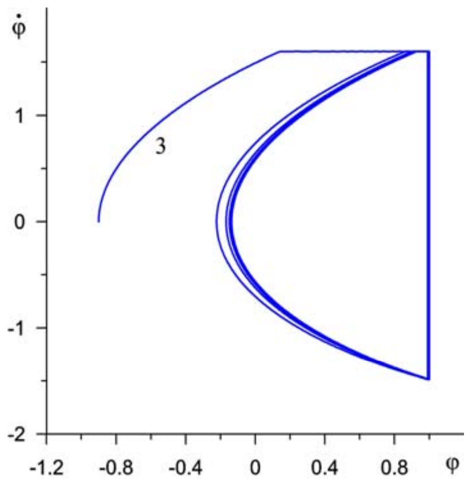


Fig. 7. Phase trajectory of the bush movement for $\gamma_1 = 0.1$ , $k^w = 0$

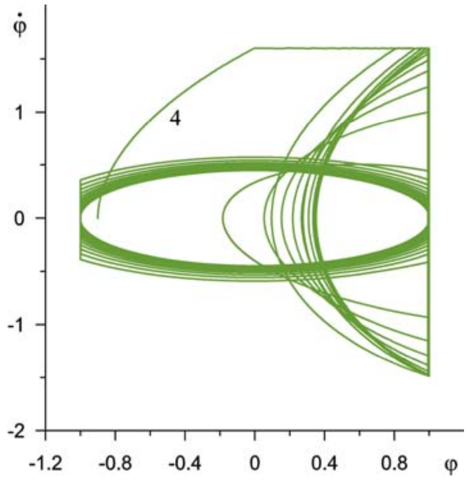


Fig. 8. Phase trajectory of the bush movement for $\gamma_1 = 0.5$ , $k^w = 0.02$

Time histories of contact pressure, temperature on surface contact and wear are reported in Figure 9-11. Curves 1 correspond to the case when $\gamma_1 = 0$ (lack of heat extension), $k^w = 0$ (lack of bush wear). Curves 2 correspond to the case of heat transfer lack ( $\gamma_1 = 0$ ) and $k^w = 0.02$ (heat generation included). Curves 3 correspond to the case where the shaft heat expansion is taken into account ( $\gamma_1 = 0.1$ ), but the bush wear is neglected ( $k^w = 0$ ). Curves 4 correspond to the case where both mentioned parameters are taken into account ( $\gamma_1 = 0.5$ , $k^w = 0.02$ ).

In the first case ( $\gamma_1 = 0$ , $k^w = 0$ ), where the tribological processes are not taken into account the phase curve approaches a stable orbit (curve 1 in Figure 5). In this case the contact pressure is exhibited by curve 1 in Figure 9.

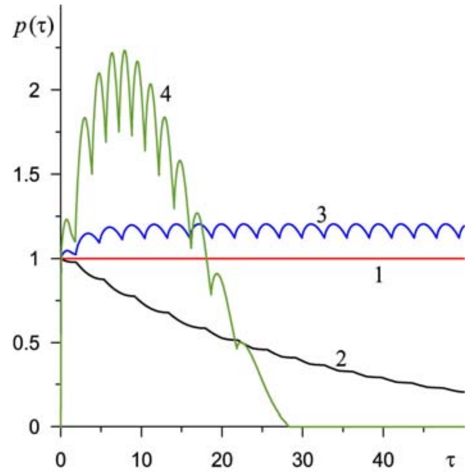


Fig. 9. Time histories of dimensionless contact pressure $p(\tau)$ versus dimensionless time $\tau$ for different values of $\gamma_1$ and $k^w$

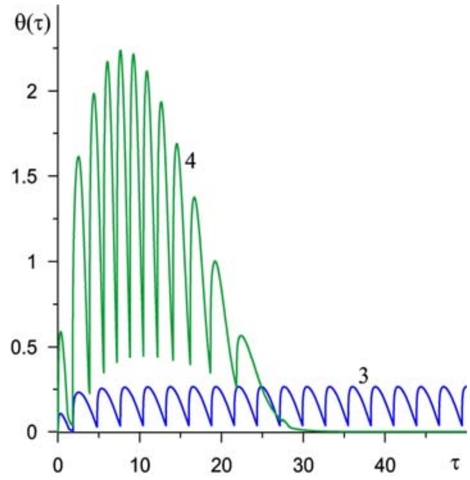


Fig. 10. Time histories dimensionless contact temperature $\theta(1,\tau)$ versus dimensionless time $\tau$ for different values of $\gamma_1$ and $k^w$

The bush wear ( $\gamma_1 = 0$ , $k^w = 0.02$ ) occurrence decreases the contact pressure (curie 2 in Figure 9), which tends to zero value (the corresponding phase curve is shown in Figure 6). Note that after the wear process, the bush moves in a periodic manner. Bush wear kinematics is shown in Figure 11 (curve 2).

An inclusion of the shaft heat expansion ( $\gamma_1 = 0.1$ ) within the given heat transfer conditions ( $Bi = 10$ ) yields a periodic change of both contact pressure (curve 3 in Figure 9) and temperature (curve 3 in Figure 10). The phase curve after a transitional process tends to a new stable periodic orbit (curve 3 in Figure 7). For a general case, i.e. where the tribological processes are taken into account ( $\gamma_1 = 0.5$ , $k^w = 0.02$ ) and for the given heat transfer conditions ( $Bi = 10$ ) the obtained results are exhibited by curves 4 in Figures 8-11. In this case the bush wear increase owing to the shaft heat extension, and the contact pressure first increases and then it tends to zero (curve 4 in Figure 9). The contact temperature being changed in an oscillatory manner periodic first increases, but then decreases with decrease of the contact pressure. The Bush wear kinematics is exhibited by curie 4 in Figure 11. Observe that the final wear amount is larger than the initial shaft compression. In this case the phase curve (after the bush is wear) approaches a stable periodic orbit (curve 4 in Figure 8).

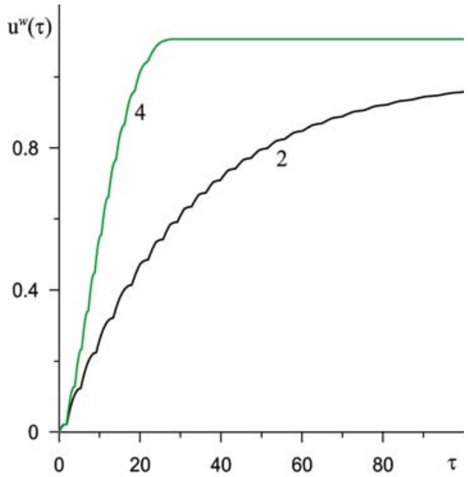


Fig. 11. Time histories of dimensionless wear $u^w(\tau)$ versus dimensionless time $\tau$ for different values of $\gamma_1$ and $k^w$

In the case when the bush wear is less than the shaft thermal expansion (for instance in the case of $\gamma_1 = 1$ , $Bi = 10$ ), the contact characteristics increase in an exponential manner with time increase. In the latter case the shaft can not succeed in making cooling in time.

## V. Conclusion

We have proposed a novel model of vibrations of the bush-shaft system with inclusion of both impacts and tribological processes occurring on the contact surface. A similar system, however without impacts, has been studied earlier by the authors and it has been described in references [2], [3]. The occurrence of self-excited vibrations in a more simplified system with a gap (without tribological processes and springs) has also been analyzed in reference [7], [8].

Applying the Laplace transformation, our problem has been reduced to that of the system of one non-linear differential equation and one second-order Volterra integral equation with respect to the contact pressure. A kernel of the latter equation is the function of the sliding velocity. Note that the change of the bush rotational speed, contact pressure, surface contact temperature and wear are mutually dependent. We have estimated analytically the restitution coefficient for which a periodic motion appears assuming small slope of friction characteristics. We have shown, among the others, various periodic motions exhibited by the analyzed system and we have verified numerically our theoretical considerations and predictions.

For an arbitrary restitution coefficient $k^* \in (k_{\min}, 1)$ two periodic orbits (stable and unstable) appear on the phase plane. Increase of the parameter $k^*$ from $k_{\min}$ to 1 yields increase (decrease) of stable (unstable) periodic orbit. For $k^* = 1$ the unstable periodic orbit is reduced to the point $(1, 0)$. Decrease of the parameter $k^*$ causes approaching of both stable and unstable periodic trajectories. For $k^* = k_{\min}$ a bifurcation occurs and a halfly-stable periodic orbit is born substituting two previous stable and unstable orbits. In other words for $k < k_{\min}$ a periodic motion is not exhibited by the studied system.

The final conclusion follows: Tribologic processes has an important impact on the studied system dynamics, since they may change it even qualitatively.

## VI. Acknowledgement

This work has been financially supported by the Polish Ministry of Education and Science for the years 2005-2008 (grant No. 4 TO7C 044 29).

## References

[1] Awrejcewicz J. and Lamarque C. –H. *Bifurcation and chaos in nonsmooth mechanical system.* Vol. 45 Series A. World Scientific, New Jersey, London, Singapore, 2003.

[2] Awrejcewicz J. and Pyryev Yu. Thermoelastic contact of a rotating shaft with a rigid bush in conditions of bush wear and stick-slip movements. *International Journal of Engineering Science*, 40 : 1113-1130, 2002.

[3] Awrejcewicz J. and Pyryev Yu. Contact phenomena in braking and acceleration of bush-shaft system. *Journal of Thermal Stresses*, 27(5) : 433–454, 2004.

[4] Nowacki W. *Thermoelasticity*. Pergamon Press, Oxford, 1962.

[5] Archard J.F. Contact and rubbing of flat surface. *Journal of Applied Physics*, 24(8) : 981-988, 1953.

[6] Carslaw H.S. and Jaeger J.C. *Conduction of Heat in Solids*. Clarendon Press, Oxford, 1959.

[7] Balandin, D.V. Frictional vibrations in a gap, *MTT*, 1 : 54-60, 1993, in Russian.

[8] Filippov A.F. *Differential equations with discontinuous right-hand sides. In Mathematics and Its Applications*. Kluwer Academic, Dordrecht, 1988.